TERAHERTZ IMAGING, MILLIMETER-WAVE RADAR

R. W. McMillan
U.S. Army Space and Missile Defense Command
Huntsville, Alabama, USA

Abstract The millimeter wave (MMW) band of frequencies extends from 30 GHz to 300 GHz, with some fuzziness on both ends of this spectrum. The terahertz (THz) band extends from about 200 GHz to about 30 THz, despite the fact that the lower frequencies in this range are not strictly 10^{12} Hz or higher. These bands are also variously called submillimeter, far-infrared, and near-millimeter. In recent years, there has been some degree of hype associated with the capabilities of systems operating in these bands. Sometimes exorbitant claims have been made relative to the ability of these systems to see through walls, detect buried structures, and detect cancer cells, for example. In this chapter we shall examine some of these clams and assess their validity. We shall find that MMW and THz systems can do some amazing things, some of them not related to the above claims, and that there is substantial promise of even more interesting results. In this chapter we begin by discussing these atmospheric limitations, since they permeate the whole technology of MMW, sub-MMW, and THz technology. We then discuss MMW and THz sources, detectors, optics, and systems in separate sections. Finally, we present some results obtained using sensors operating in these bands. Perhaps the most interesting of these results demonstrate the capability to image objects at resolutions as good as $\lambda/100$, where λ is wavelength. These measurements show the connection between this sensor technology and applications to security.

1. Introduction

Electromagnetic radiation in the range of wavelengths from 1 cm to 1 mm is characterized as millimeter-wave (MMW) radiation, while the range extending from 1 mm to 0.3 mm is called sub-millimeter wave (sub-MMW or sub-mm), and that of shorter wavelengths extending to the infrared is terahertz (THz) radiation. From the opticist's point of view, the latter range is also known as the far-infrared (far-IR) range. From a very practical aspect, these ranges have traditionally overlapped.

For example, many workers in the field consider that the MMW band begins at 40 GHz (7.5 mm) because of the similarities in systems and components in Ka-band (26.5–40 GHz) to those of the microwave bands. Similarly, because of the difficulty in generating and detecting THz signals, this band is sometimes considered to begin at frequencies variously extending from 200 to 600 GHz, depending on the worker and application involved. Indeed, most of the papers presented at THz conferences discuss systems, techniques, and results obtained in this latter band of frequencies. The far-IR band generally extends from about 20 microns (15 THz) to 0.3 mm (1 THz).

System development and operation at frequencies above about 300 GHz are usually confined to passive applications such as radio astronomy and remote sensing using radiometry because of the difficulty in generating usable amounts of power at these frequencies. It is not particularly difficult to generate the small amount of power useful for pumping a THz mixer, however, so that many passive applications are found in this range. This limitation is being overcome to a large extent by continuing research in this area. Another limitation on performance of systems at these higher frequencies is the absorption in the atmosphere, mostly due to water vapor, which begins to limit transmission severely above about 300 GHz.

In this chapter we begin by discussing these atmospheric limitations, since they permeate the whole technology of MMW, sub-MMW, and THz technology. We then discuss MMW and THz sources, detectors, and systems in separate sections. Finally, we present some results obtained using sensors operating in these bands. These results show the connection between this sensor technology and applications to security.

2. Atmospheric Limitations

The atmosphere is the most significant factor in limiting the performance of MMW and THz systems. The characteristics of the atmosphere that cause this limitation are attenuation and turbulence, and attenuation is much more significant than turbulence. There are regions of the spectrum in these bands that are attenuated by as much as 500 dB/km, which makes operation at ranges of even a few meters extremely challenging. Atmospheric turbulence causes fluctuations in signal intensity of 2–3 dB and changes in angle-of-arrival of several tens of microradians. Each of these effects is discussed in more detail in the following paragraphs.

Perhaps the most useful calculations of atmospheric attenuation have been done by Liebe [1], who used a variant of the Van Vleck-Weisskopf

(VVW) [2] equation for the line shapes of water vapor and other atmospheric constituents. It is a common practice in calculating atmospheric attenuation to add a frequency-dependent empirical correction factor to the calculation because none of the analytic line shapes developed thus far give accurate results in the atmospheric window regions. Based on the VVW line shape, this correction factor, and his own measurements [3], Leibe has developed a computer program called MPM [4] that calculates attenuation as a function of a variety of factors including temperature, pressure, and relative humidity as well as for a number of other conditions such as rain and fog. MPM has been shown to give results accurate to about 0.2 dB/km in the atmospheric window regions of interest in the range 0–1000 GHz. Figure 1 shows the results of calculating the atmospheric attenuation over the range 40–1000 GHz for relative humidities of 50 and 100 percent and rainfall rates of 5 mm/h and 20 mm/h. The curve for 100 percent relative humidity includes attenuation due to 0.5 g/m3 of condensed water vapor, corresponding to a fog that would give only 100 m visibility in the visible spectrum. Note that this thick fog does not greatly affect propagation, especially at the lower frequencies, because attenuation due to fog results mainly from Rayleigh scattering in these bands. Rainfall is another matter, however. Raindrop size distribution depends strongly on rain rate; larger drops occur at higher rain rates. Since raindrops are on the order of a few millimeters in diameter, strong attenuation due to Mie scattering occurs. The rainfall curves of Figure 1 show that the Mie resonance occurs in this region, corresponding to maximum Mie scattering. After the frequencies due to Mie resonance have been exceeded, Mie scattering remains almost constant well into the visible range.

It is a bit surprising that atmospheric turbulence affects propagation at MMW and THz frequencies, since it has been shown theoretically [5] and verified experimentally [6] that the log amplitude variance of amplitude fluctuations varies as f7/6 where f is frequency. These effects are strong at visible and infrared wavelengths, where frequencies are two orders of magnitude higher, so one would expect that they would be minimal at 1 THz. The answer to this question lies in the fact that the atmospheric turbulence structure parameter, commonly denoted as Cn2, is much larger, sometimes as much as two orders of magnitude, at MMW and THz frequencies because of the contribution of water vapor at these latter frequencies [7]. This parameter, which includes contributions from temperature and water vapor, as well as the cross-correlation of these two parameters, occurs in all computations of atmospheric turbulence effects including both intensity and phase fluctuations. Figure 2 shows the results of measuring fluctuations in the intensity of a 140

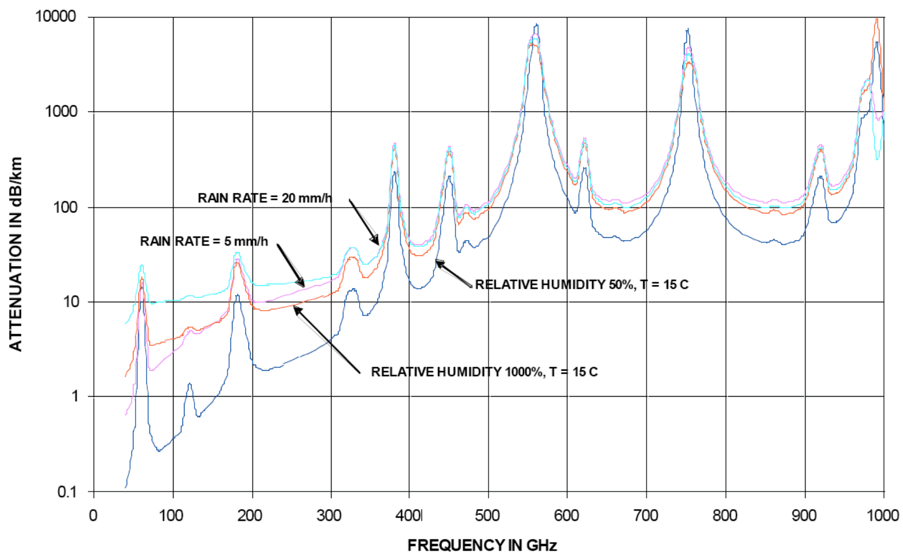

Figure 1. Atmospheric attenuation in the range 40–1000 GHz

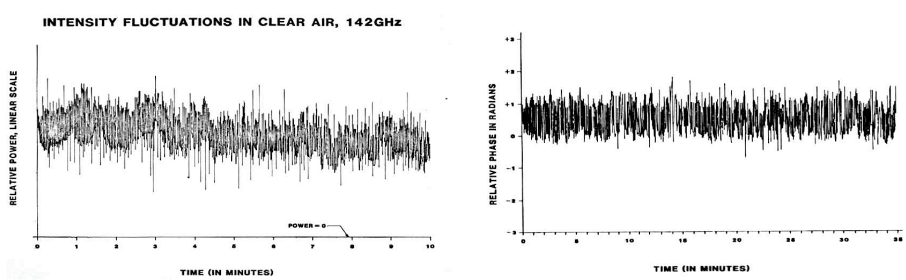

Figure 2. Intensity and phase fluctuations measured over a 1.3 km path at the same time

GHz signal propagated over a range of 1.3 km at a very flat site near Champagne-Urbana, IL [6]. Figure 2 shows the corresponding phase fluctuations. These results were obtained on a hot and humid summer day, which is the worst-case condition for turbulence effects at MMW frequencies. Observations in snow, rain, and fog all gave smaller fluctuations, even though the signals propagated through rain showed strong, comparatively long-term changes due to variations in rain rate during the observation time.

3. Millimeter-Wave and Terahertz Sources of Radiation

As frequency increases, it becomes increasingly difficult to generate radiation at usable power levels. This limitation is due to the decreasing size of the frequency-sensitive elements in most sources of radiation. In general, the frequency-sensitive elements decrease in size linearly with wavelength. At the higher frequencies, it becomes more difficult to fabricate these small structures with accuracy good enough to ensure good performance. This problem occurs with both solid-state and tube-type sources of radiation.

Exceptions to this general rule are the so-called beam wave tubes and optically-pumped lasers. The gyrotron and the free-electron laser (FEL) are example of beam-wave tubes. The gyrotron uses stimulated cyclotron emission of electromagnetic waves by electrons [8]. This tube is an axially symmetric device having a large cathode, an open cavity, and an axial magnetic field. Electrons are emitted from the cathode with a component of velocity perpendicular to the magnetic field, so that they are caused to spiral as they are accelerated through the magnetic field to the collector. This spiraling occurs at the cyclotron frequency of the electrons, and it is this frequency that is radiated by the tube. The coupling between the electron beam and the MMW radiation allows the beam and microwave circuit dimensions to be large compared to a wavelength so that the power density and related circuit dimension problems encountered in almost all other MMW tubes are avoided. Power outputs of 22 kW CW at 2 mm and 210 kW pulsed at 2.4 mm have been obtained. Because of this high power, gyrotrons are used for such applications as plasma heating in fusion experiments and for extremely high power radars. Russian scientists have built a megawatt radar operating at Ka-band using an array of gyrotrons [9]. This system uses multiple power-combined gyrotrons and multiple Cassegrain antennas in a phased-array configuration.

FELs use relativistic electron beams propagated through a periodic structure of magnets, called an undulator, to generate radiation over a broad spectrum from the submillimeter wave to the x-ray region. These systems are extremely large and are placed in permanent installations. They are used for remote sensing and materials testing over a broad range of wavelengths.

Optically-pumped lasers (OPLs) offer very useful power levels at discrete frequencies well into the THz band. Most OPLs comprise some sort of gas cell, which is the active laser medium, that is pumped by a carbon dioxide laser. These devices are inherently inefficient because the pump laser excites the active medium into a higher vibrational state, and the laser transitions occur between rotational levels within this state, an energy difference of several orders of magnitude. Both CW and pulsed OPLs have been built at thousands of different wavelengths within the MMW and THz bands. They are not useful for many applications because they operate only on discrete frequencies and because the pulsed versions have low duty cycle.

A family of vacuum-tube MMW sources is based on the propagation of an electron beam through a so-called slow-wave or periodic structure. Radiation propagates on the slow-wave structure at the speed of the electron beam, allowing the beam and radiation field to interact. Devices in this category are the traveling-wave tube (TWT), the backward-wave oscillator (BWO) and the extended interaction oscillator (EIO) klystron. TWTs are characterized by wide bandwidths and intermediate power output. These devices operate well at frequencies up to 100 GHz. BWOs, so called because the radiation within the vacuum tube travels in a direction opposite to that of the electron beam, have very wide bandwidths and low output powers. These sources operate at frequencies up to 1.3 THz and are extensively used in THZ spectroscopic applications [10–12]. The EIO is a high-power, narrow band tube that has an output power of 1 kW at 95 GHz and about 100 W at 230 GHz. It is available in both oscillator and amplifier, CW and pulsed versions. This source has been extensively used in MMW radar applications with some success [13].

A variety of solid-state sources operate in the MMW portion of the spectrum with varying power outputs and bandwidths. Gunn oscillators, which are bulk devices made from GaAs, InP, and GaN, are available at frequencies of up to 140 GHz in the InP version and may serve as oscillators in the THz region [14]. These oscillators operate based on the negative resistance caused when carriers are excited from a higher mobility to a lower mobility state by the application of an electric field. Gunn devices have outputs of a few milliwatts and are low-noise devices, so that they are useful as local oscillators in MMW receivers. Impact-Ionization Transit-Time (IMPATT) oscillators have higher output powers than Gunns, but have higher noise outputs as well because of the way in which carriers are generated. Carriers are generated in a semiconductor by impact ionization. These carriers traverse a drift region with some transit time. Because of the transit time, the current through the device lags the voltage, and when this lag exceeds 90 degrees, oscillation will occur. Both Gunns and IMPATTs have been supplanted for many applications, especially at lower frequencies, by field-effect transistors (FETs). The great advantage of FETs in circuit applications is that they are three-terminal devices and this third terminal is a gate by which the gain of the device can be controlled. FETs are used in low-noise amplifier applications up to 100 GHz and in power amplifier applications to about 40 GHz. FETs can be integrated into circuits with other functions so that they are very useful in radar transmit-receive modules, but so far this application is limited to the microwave frequencies. FET oscillators have operated at frequencies up to 230 GHz. Solid-state devices suffer from the same decrease in size of the frequency-determining elements as do vacuum tubes, so that solid-state device operation is limited to about 230 GHz.

The above discussion indicates that the only fundamental source available in the THz spectral region is the BWO. For many years before these tubes became available, molecular spectroscopists relied on generating power by multiplying the output of a lower-frequency source. This technique is still used extensively today. Frequency multiplication is based on irradiation of a nonlinear device, such as a varactor, with a lower frequency. The varactor generates multiple harmonics because of its nonlinearity, and powers at the desired frequencies are enhanced by careful cavity design. Since the input frequency is multiplied, the bandwidth of the input signal source is multiplied by the same factor. In the THz band, power outputs of only a few microwatts are generated, but these levels are enough for many spectroscopic applications. Figure 3 is a photograph of a varactor-based multiplier capable of output in the range 1.26–1.31 THz at a level of 10 (W with an input of 1 mW at 18 GHz [15]. This power level is useful for spectroscopic measurements.

4. Millimeter-Wave and Terahertz Detectors and Receivers

The earliest detectors of MMW and THz radiation, and indeed of microwave radiation in general, were simple point-contact diodes made by carefully contacting a crystal with a sharpened wire, or "cat's whisker". This technique is still used for the higher frequencies today and is still a very useful and effective method of detecting radiation at frequencies into the visible range. It has been refined in recent years by the use of Schottky-barrier structures in which a GaAs semiconductor crystal is contacted through gold contacts set in a mask of insulating SiO2. These diodes have very low stray capacitance and operating frequencies extending well into the THz range. An interesting and perhaps surprising detector comprises a tungsten cat's whisker contacting a metal oxide layer on a metal post, such as aluminum [16]. This so-called metal-oxide-metal (MOM) diode has been used in mixing experiments for lasers

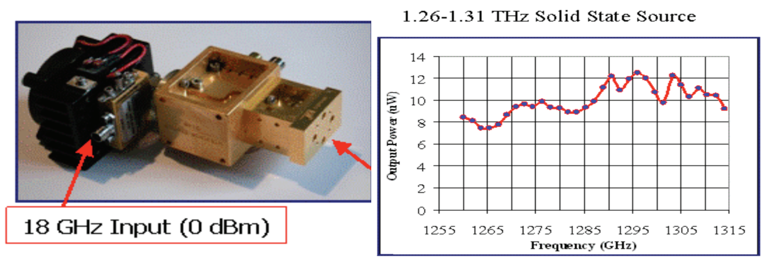

Figure 3. A varactor doubler with output in the THz spectrum [15]

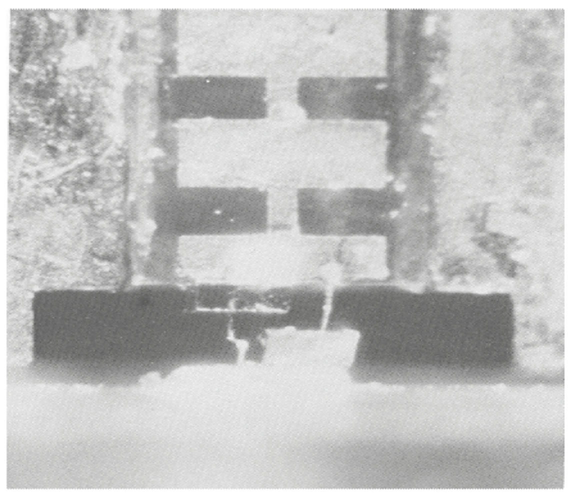

Figure 4. Back-to-back point contact diodes in a subharmonic mixer configuration

operating into the visible spectrum and has been used for very precise measurements of the speed of light [17]. Figure 4 is a photograph of such a diode contact, and Figure 5 shows an array of gold windows in an insulating mask on GaAs that is used to form Schottky barriers.

An interesting variant of the point-contact mixer is the back-to-back diode configuration in which the fundamental frequency and all odd harmonics are cancelled, resulting in a mixer that operates at twice the fundamental [18], and in some cases at four times the fundamental [19]. This configuration has been used to extend the range of all operational solid-state receivers to 320 GHz and higher. Figure 6 [15] shows a 320 GHz receiver with a system noise temperature of 1360 K built using this technique.

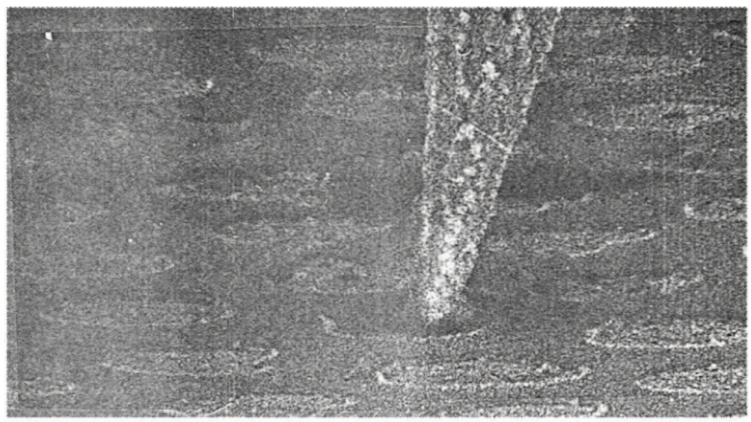

Figure 5. Photograph of a point-contact Schottky-barrier diode. The magnification is about 11,000 times

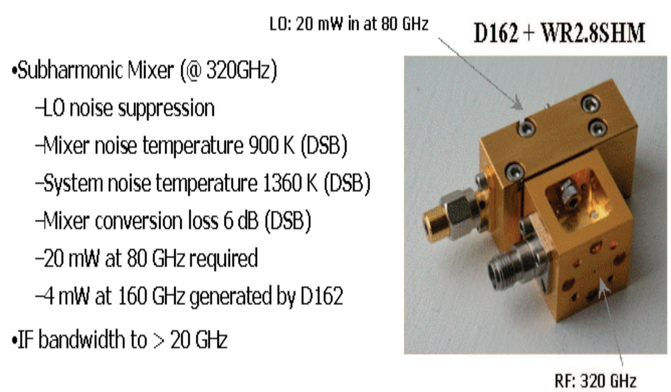

Figure 6. A 320 GHz receiver based on a subharmonic mixer [15]

The ability to make ever smaller solid-state devices by improved lithography techniques has led to the development of so-called beam lead Schottky-barrier diode detectors and mixers in which diodes are fabricated by the same techniques used to make integrated circuits, and for this reason, they can be included in these circuits. Figure 7 shows such a beam-lead detector/mixer made by Virginia Diodes of Charlottesville, VA [15]. This same configuration is used in fabricating the varactor devices used for frequency multiplication discussed in the preceding section.

A significant gap in detector coverage exists in the range extending from about 1 THz to 6 THz (300 m to 50 m wavelength). This band can be covered by the MOM devices mentioned above, but they are too noisy and fragile for most applications. Radio astronomers have long used cryogenically-cooled detectors such as Josephson junction devices for this region [20]. Another possibility for some needs is the uncooled bolometric detectors made from barium strontium titanate, for example, and designed for operation in the long-wave infrared band [21]. Significant progress has been made in the development of these detectors to the extent that they are extensively used for both civilian and military imaging purposes. They have demonstrated minimum detectable temperature differences of as low as 50 mK in the long-wave infrared band. Unfortunately, their use in the far-infrared and THz regions of the spectrum is limited because of the rapid rolloff in energy output from a room-temperature black body in the THz bands. These devices have the overwhelming advantage of being available in imaging arrays, so that numerous security related issues needing imaging sensors can be addressed.

5. Millimeter-Wave and Terahertz Optics

At frequencies above about 100 GHz, and at lower frequencies for many applications, metal waveguides become unacceptably lossy because of skin effect losses and our inability to make these waveguides with the precision required for low-loss operation. In many cases, these problems can be solved by using techniques developed for the visible and infrared portions of the spectrum. This approach to the propagation and handling of MMW and THz radiation has been called "quasi-optics" or "diffraction-limited optics". The latter term arises because the approximations of geometrical optics, namely infinitesimally small focal points and perfectly collimated beams, no longer apply. Instead, beams are focused to spot sizes depending on wavelength, distance, and aperture size, and collimated beams undergo significant diffractive spreading.

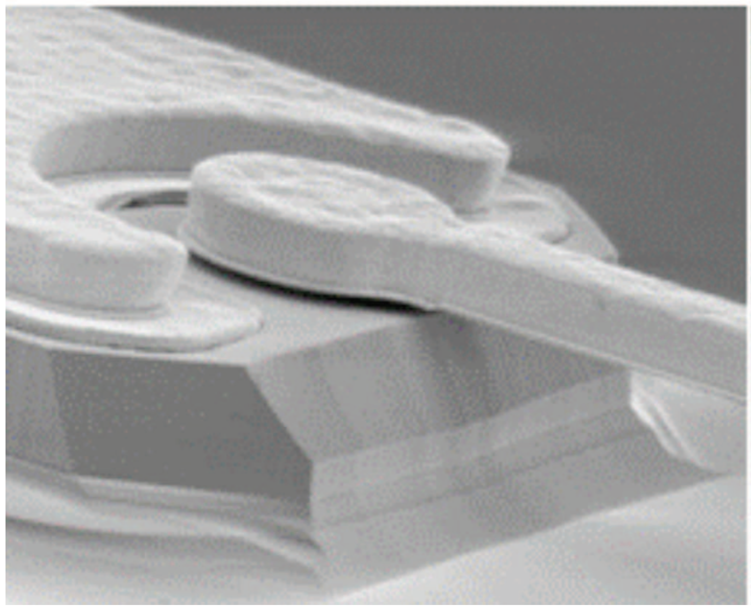

Figure 7. A beam-lead Schottky-barrier detector/mixer [15]

It is possible to build optical analogs of almost all waveguide components including waveguides, attenuators, polarization rotators, directional couplers, and antennas. For example, Figure 8 shows a section of optical beam waveguide that is analogous to metal waveguide. The difference is that the optical waveguide will operate at much higher power levels and at much lower loss than the metal waveguide. The only significant loss in the optical waveguide is the reflection loss at the lens interfaces caused by the index of refraction of the lens material. This loss can be corrected by machining radial grooves into the lenses that are one-quarter wavelength in depth and with an aspect ratio such that the average index of the machined area equals the square root of the index of the lens material. Essentially zero loss, together with high power handling capability, can be achieved if the beam waveguide is made from mirrors. Two disadvantages of beam waveguides, and of MMW and THz optical components in general, are that these devices are bulky, and they may require mode converters if it is necessary to convert to the fundamental waveguide mode.

Many common plastic materials can be used to make useful MMW and THz optical components. Lenses can be machined on a lathe, and the exact desired hyperbolic figure can be obtained to avoid spherical

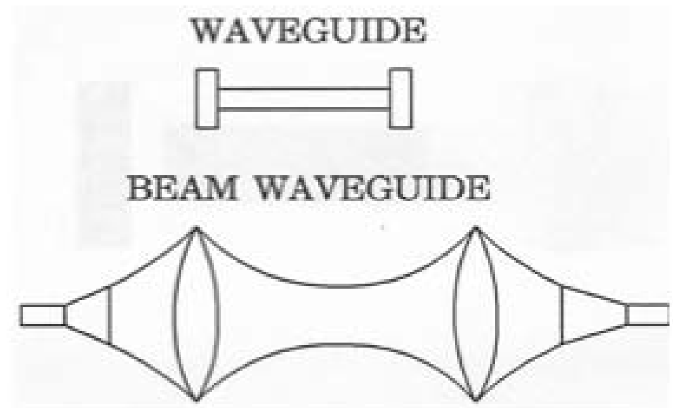

Figure 8. MMW/optical analog—waveguide/beam waveguide

aberrations. Some plastics have the advantage of good transmission in the visible as well, so that visible images can be used for rough alignment of MMW optical systems. Crystalline quartz and sapphire are very useful materials in these ranges, since they have good transmission from about 20–50 microns to very long wavelengths. These materials can often be anti-reflection coated with plastics such as MylarR, since the indices of refraction of many plastics is roughly equal to the square root of the indices of quartz and sapphire. For example, MylarR, with an index of 1.7, is useful for AR coating sapphire, with an average index of 3.24. Both sapphire and quartz are birefringent, so that they are useful for fabricating wave plates at MMW and THz frequencies. The 225 GHz radar discussed in a later section used a quarter-wave plate to give a circularly-polarized output as part of a polarization duplexer. This radar used several other optical components including lenses and polarizing beam splitters.

The examples given in this section are just a few of the many applications of optical techniques in the MMW and THz bands. It would not be possible to build many systems in these bands without using optical techniques.

6. Millimeter-Wave and Terahertz Systems

The MMW and THz spectral bands are rich in phenomenology including those phenomena related to security applications. Although this region has long been the province of a few specialists seeking to learn more about physics-related problems, in recent years enough progress has been

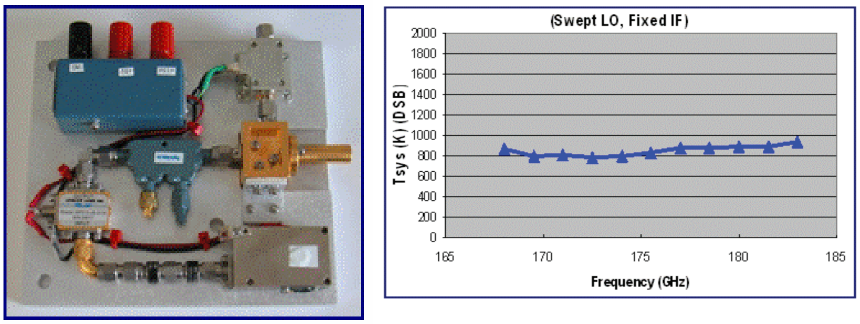

Figure 9. A 183 GHz receiver and its system noise temperature as a function of frequency [15]

made in sources and detectors that useful sensor systems are beginning to be available. In general, this progress has proceeded from the lower frequencies upward using extensions of the lessons learned by developing systems at the microwave and lower MMW frequencies. Recently, more progress has been made in moving downward from the visible/infrared spectral regions through the more extensive use of so-called quasi-optical or diffraction-limited optical techniques [22].

One of the earliest applications of MMW technology to practical needs was in the use of radiometers for atmospheric temperature and water vapor sounding and sea-ice detection. An early radiometer developed for the National Aeronautics and Space Administration (NASA) by Georgia Tech [23] operated in an atmospheric transmission window at 91.5 GHz for sea-ice sensing and on the strong atmospheric water-vapor absorption at 183 GHz for water vapor sounding. This device used a single klystron local oscillator at 91.5 GHz for both receivers. Its output was doubled for the water vapor sensor. A later version of the 183 GHz radiometer used back-to-back point-contact Schottky-barrier diodes in a X2 subharmonic mixer configuration [18]. Figure 9 shows an all solid-state 183 GHz mixer that has a system noise temperature of only 800 K [15]. Figure 10 shows a 94 GHz MMW image obtained from a scanning radiometer that clearly shows two handguns hidden beneath a person's sweater. One of these guns is made primarily of plastic. This latter image illustrates one application of MMW technology to security needs [24].

There are few examples of mass produced MMW radars used for either commercial or military applications. An exception is the US Army's Longbow Apache attack helicopter that is equipped with the Northrop Grumman MMW Longbow radar. The Longbow fire control radar incorporates an integrated radar frequency interferometer for passive location

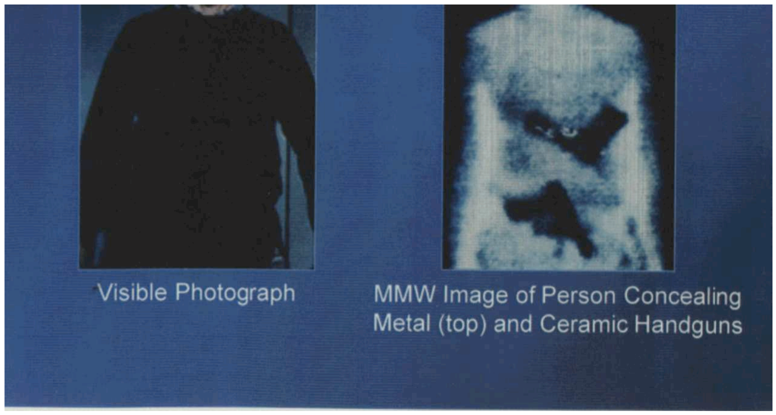

Figure 10. A 94 GHz image of a person concealing two handguns beneath a heavy sweater [24]

and identification of radar emitting threats [25]. The obvious advantages of MMW radar for this application are that the antenna can be made small, and long operating range is not needed.

MMW radars have been designed primarily for remote sensing or one-of-a kind evaluation in military applications. Such systems have been built in the atmospheric windows near 95, 140, and 230 GHz. Figure 11 is a photograph of a radar that operates at 225 GHz that was built for the US Army at Georgia Tech [19]. This radar used some unique techniques in its design, including an all solid-state receiver using an f/4 subharmonic mixer pumped by a 55 GHz Gunn oscillator, a 60 W pulsed extended interaction oscillator (EIO) klystron transmitter, and a quasi-optical polarization duplexer employing a sapphire quarter-wave plate. This radar employed the first all solid-state receiver built at 225 GHz and was the first radar at this frequency to be phase locked. A unique intrapulse feedback phase locking scheme was used to phase lock the EIO transmitter, making this radar the highest frequency microwave coherent radar built up to that time. Figure 12 is a chart showing Doppler returns from a tank measured with this system. The chart clearly shows Doppler returns from the tank body as well as from its treads.

The most common application of MMW systems to security needs is the MMW radiometric imager. Systems of this type are very useful because of their ability to detect a variety of concealed weapons hidden by clothing. Millivision Technologies of South Deerfield, MA has been a leader in this field by developing a family of imagers that operate in the 94 GHz atmospheric window and that use a superheterodyne receiver

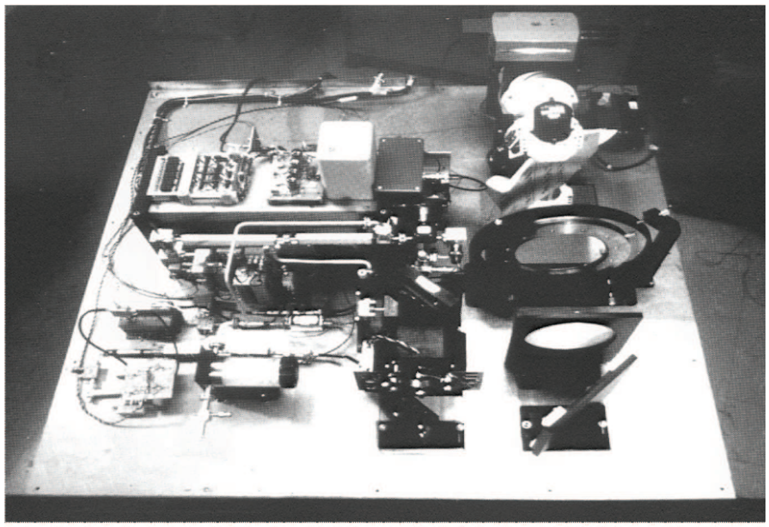

Figure 11. A 225 GHz pulsed coherent radar

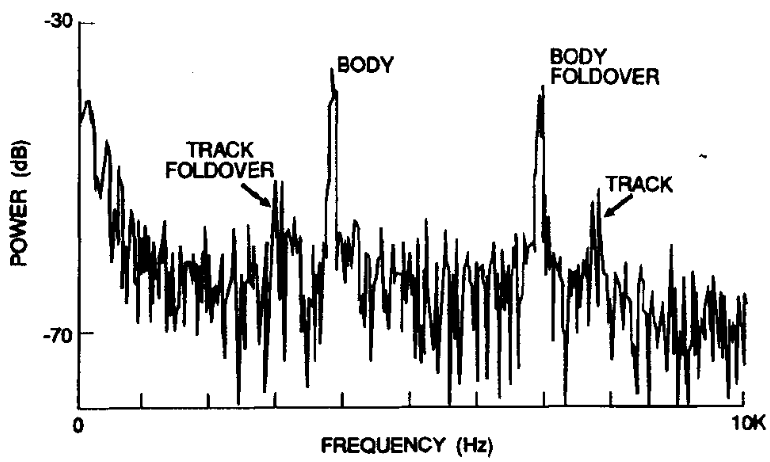

Figure 12. Doppler returns from a tracked vehicle measured by the 225 GHz radar described in the text

Figure 13. The Millivision Vela 125 MMW imager and its specifications

for improved sensitivity. A commercial imager developed by Millivision, the Vela 125, has a thermal sensitivity of 1 K at 1 Hz frame rate and 3 K at 10 Hz frame rate [26]. Such imagers operate on the principle that a metal weapon will reflect the temperature of the ambient surroundings, nominally at 300 K, and the human body is a good emitter at 310 K. This contrast of 10 K is easily detected by a radiometer such as the Vela 125 and weapons can be readily recognized if the radiometer has sufficient spatial resolution. Figure 13 is a photograph of the Vela 125 [26].

A MMW imager that uses a unique pupil plane array of sensors has been built by ThermoTrex of San Diego, CA. This device uses a vertical array of slotted waveguide antennas in an aperture of about one square meter. Horizontal resolution is achieved by the vertical array spacing, and vertical resolution by the characteristic of a slotted antenna whereby the sensitivity of the antenna at a given frequency is a function of angle. This sensor also operates at 94 GHz. Figure 14 [27] is an image of a group of persons, one of whom is concealing a weapon beneath clothing, made with this imager. A visible image is also shown.

A 94 GHz MMW imaging radar for aircraft landing operations in poor weather has been designed and built by BAE Systems (formerly Lear Astronics) of Ventura, CA [28]. This instrument has been extensively tested on Air Force airplanes and has been shown to provide useful landing information in weather conditions below normal minimums. This imager uses a scanned range-crossrange radar format with a single detector. It operates on the principle that radiation from the radar in-

Figure 14. Visible and MMW images of a group of persons, one of whom is concealing a simulated handgun [27]

cident on a runway is forward-scattered because of the oblique angle of incidence, while radiation incident on adjacent grassy surfaces is more strongly backscattered to the radar. Smooth surfaces such as runways and taxiways appear to be light-colored in the image, while surrounding areas are dark, thus providing good contrast.

A passive MMW imaging system using monolithic microwave integrated circuit (MMIC) amplifiers on its front end is being developed by Velocium, a subsidiary of Northrop Grumman, formerly TRW, of Redondo Beach, CA [29]. This instrument is also being developed for aircraft landing systems. It uses a single MMIC amplifier operating at a center frequency of 89 GHz with a 10 GHz bandwidth for each pixel of the target scene. The advantage of this imager is that its minimum detectable temperature is determined by the noise figure of the MMIC amplifier and not by the conversion loss of a mixer normally used on the front end of such an imager.

MMW and THz measurement systems have been developed to sense a wide range of features including the MMW turbulence sensing system described in the section on atmospheric limitations [7]. Other applications include the radiometer for sensing sea ice, described above in this section and other sensors designed to detect ice on the space shuttle external tanks. These measurement systems are necessarily limited in wavelength to that range of wavelengths that propagates more or less readily through the atmosphere. A sensor for the remote sensing of wind shear and clear-air turbulence has been proposed by McMillan [30]. This instrument would operate at the center of the group of atmospheric oxygen absorption lines centered at 60 GHz. Several radiometer channels can be processed to detect the temperature of the atmosphere remotely. Since atmospheric hazards are known to be associated with temperature fluctuations, they can be remotely sensed by this method. A similar method is used to sense the atmospheric water vapor profile from high altitudes or from space. In this case, the sensor operates on the peak of the 183 GHz atmospheric water vapor absorption line.

THz radiometers have primarily been used for astronomical applications as noted above in the section on mixers and detectors. These devices are often based on superconducting mixers and oscillators. During the last few years, there has been some emphasis on the development of semiconductor-based THz radiometers for application in the feature-rich THz bands for remote sensing of chemical and biological agents. The development of these sensors is based on the fact that many chemical and biological agents have features in this spectral range. Efforts are being made to characterize these materials so that the proper THz frequencies can be used for sensing them. Figure 15 [29] shows the spectrum of velocities of HCO+ molecules, measured at 100 GHz, around the central black hole in the galaxy Centaurus A, superimposed on a visible image of the galaxy. These results were obtained by the Australian Radio Telescope using an InP amplifier developed by Velocium of Redondo Beach, CA.

A THz differential absorption radar has been proposed by Elliott Brown and coworkers at the University of California in Los Angeles [31]. This instrument is similar to the differential absorption lidar that has been used successfully to detect atmospheric species. Figure 16 is a block diagram of this system. A band of frequencies is transmitted through a region of interest and reflected back through this region by a retroreflector to a receiver. Differential absorption is measured as the transmitter sweeps through its range of frequencies. Despite the success of differential absorption lidar, differential absorption THz radar will have problems because of low transmitter power and relatively poor sensitivity of the available receivers. Progress is being made in the development of transmitters and receivers, however, as noted in other sections of this chapter.

A system capable of generating THz images would be of great interest for many applications because this spectral band combines the high resolution available from optical imagers with the ability to penetrate many common materials such as clothing and some building materials. An imager that would make use of the extensive uncooled focal plane array technology developed for the infrared bands has been proposed by McMillan, et al. [32]. This imager would operate in the wavelength range greater than 100 microns and would employ the bolometer detectors that have been used successfully in the long-wave infrared (LWIR) range. Among other problems with this approach is that the blackbody spectrum of a 300 K source has very little power beyond 100 microns, so

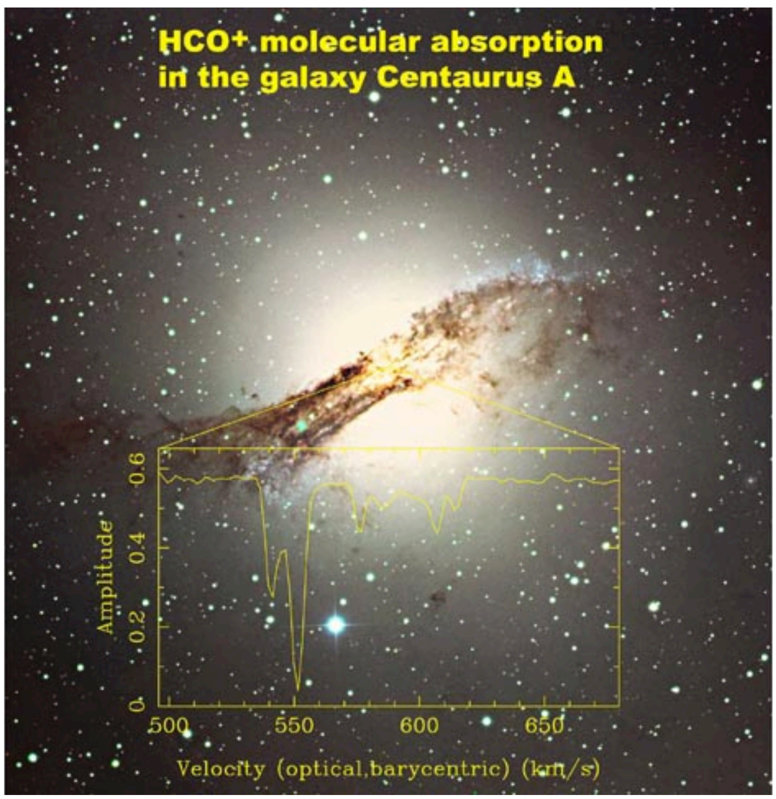

Figure 15. A spectrum indicating the velocity of HCO+ molecules around the central black hole in the galaxy Centaurus A (NGC5128) [29]. Centaurus A is the nearest galaxy containing a supermassive black hole.

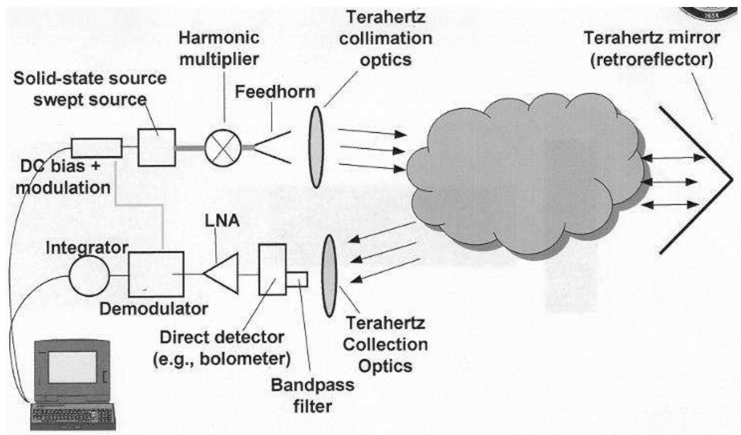

Figure 16. A differential absorption THz radar for detecting atmospheric species [31]

that some artificial means of illumination must be used. Careful analysis has shown that a liquid nitrogen cooled screen is probably the best illumination source, providing about 10 K contrast between the 300 K background and reflection of the 100 K temperature of the screen by metal objects. Another problem is the lack of lens and window materials with adequate transmission in these bands as will be discussed in the next paragraph. One of the first THz images was collected by DeLucia [33]. Figure 17 shows this image, which was collected by a scanned cooled bolometer.

In addition to the limitations imposed by low-power sources and receivers that are not sensitive, significant problems with THz materials exist. One of the most serious is the lack of window and lens materials as noted above. In the visible band, these elements can be made of quartz, glass, or clear plastic. Adequate windows for the IR bands are made of silicon or germanium. Unfortunately, these materials do not transmit well beyond about 20 microns wavelength, although quartz has good transmission beyond 100 microns and into the microwave bands. Figure 18 [34] shows the transmission of crystalline quartz in the 20–200 micron range and Figure 19 [35] shows transmission for roughly the same spectral range for high-resistivity silicon. Note that silicon is a promising material for lens and window fabrication in the far-IR spectrum. Figure 20 shows transmission of some common materials in the millimeter-wave spectrum.

Figure 17. A Terahertz image collected by a scanned cooled bolometer [33]

7. Summary

The utility of the MMW and THz spectral bands in sensing for security applications is limited by two major issues: (1) the atmospheric transmission in these bands limits their usefulness for remote sensing at ranges greater than a few meters except in a few window regions, and (2) adequate sources, detectors, and other components are not available. Paradoxically, the first issue is sometimes an advantage because absorption features in the atmosphere are used for remote sensing from high altitudes and space of water vapor and temperature profiles. For example, the 183 GHz water vapor absorption is used for water vapor profile sensing and the group of oxygen absorptions at 60 GHz is used for temperature sensing. Significant progress is being made in source and detector development driven by the need for these devices in the feature-rich MMW and THz bands. An example of source development is the discovery of a new impact ionization effect in heterojunction field effect transistors that could provide the means for developing higher-power sources in the THz spectrum [Dwight, PC]. Efforts at development of new systems and techniques in this very fruitful area of research will continue. The need for better understanding and exploitation of the MMW and THz bands is great.

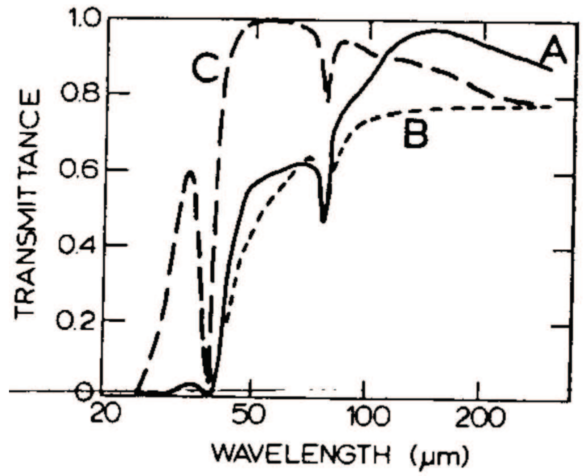

Figure 18. Transmission of crystalline quartz in the range beyond 20 microns. The A and C curves were obtained for anti-reflection coated samples and the B curve for an uncoated sample.

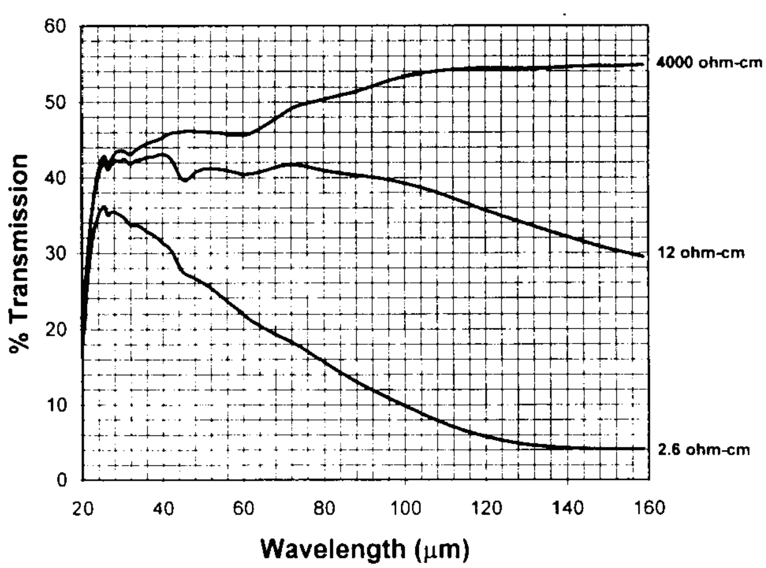

Figure 19. Transmission of high-resistivity silicon in the range beyond 20 microns. The samples are uncoated.

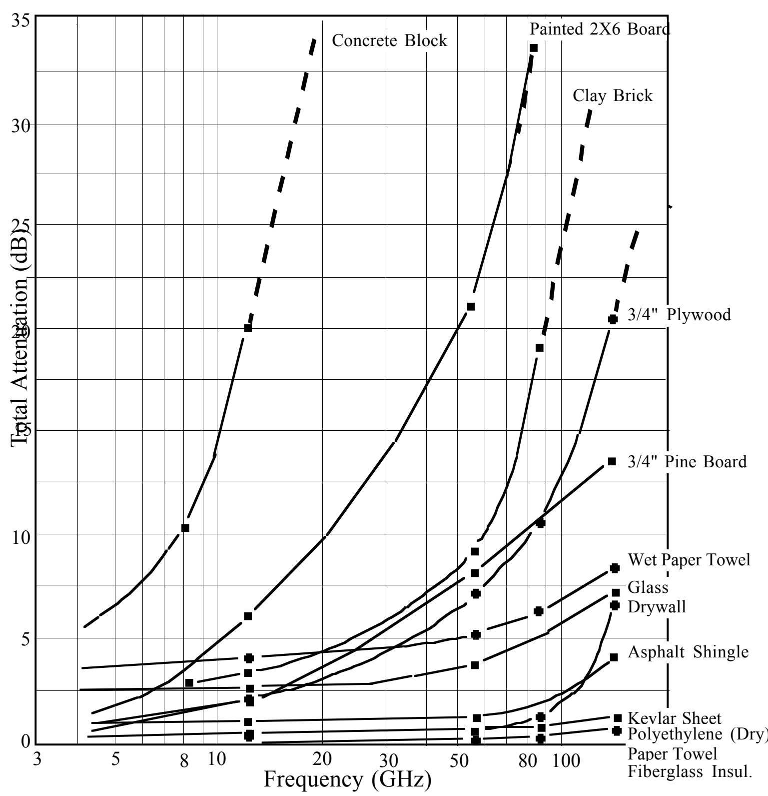

Figure 20. Attenuation of some common materials in the microwave frequency spectrum.

References

[1] K. C. Allen and H. J. Liebe. "Tropospheric Absorption and Dispersion of Millimeter and Submillimeter Waves" *IEEE Trans. Antennas Propagat.*, Vol. 31, pp. 221–223, January 1983.

[2] J. H. Van Vleck and V. F. Weisskopf. "On the Shape of Collision-Broadened Lines", Rev. Mod. Phys., Vol. 17, pp. 227–236, April–July 1945.

[3] H. J. Liebe, T. Manabe, G. A. Hufford. "Millimeter-Wave Attenuation and Delay Rates Due to Fog/Cloud Conditions", IEEE Trans. Antennas Propagat., Vol. 37, pp. 1617–1623, December 1989.

[4] H. J. Liebe and D. H. Layton. NTIA Report 87–224 National Telecommunications and Information Administration, Boulder, CO, 1987.

[5] R. S. Lawrence and J. W. Strohbehn. "A Survey of Clear-Air Propagation Effects Relevant to Optical Communications", Proc. IEEE, Vol. 58, pp. 1523–1545, 1970.

[6] R. W. McMillan, R. A. Bohlander, G. R. Ochs, R. J. Hill, S. F. Clifford. "Millimeter Wave Atmospheric Turbulence Measurements: Preliminary Results and Instrumentation for Future Measurements", Optical Engineering, Vol. 22, No. 1, pp. 32–39, January/February 1983.

[7] R. J. Hill, R. A. Bohlander, S. F. Clifford, R. W. McMillan, J. T. Priestley, W. P. Schoenfeld. "Turbulence-Induced Millimeter-Wave Scintillation Compared with Micrometeorological Measurements", IEEE Trans. Geosciences and Remote Sensing, Vol. 26, No. 3, pp. 330–342, May 1988.

[8] G.F. Brand. "Development and Applications of Frequency Tunable, Submillimeter Wave Gyrotrons", Int. J. Infrared and Millimeter Waves Vol. 16, pp. 879–887, 1995.

[9] A.A. Tolkachev, B. A. Levitan, G. K. Solovjev, V. V. Veytsel, V. E. Farber. "A Megawatt Power Millimeter-Wave Phased-Array Radar", IEEE AES Systems Magazine, pp. 25–31, July 2000.

[10] A. F. Krupnov, M. Yu. Tretyakov, Yu A. Dryagin, and S. A. Volokhov. "Extension of the Range of Microwave Spectroscopy up to 1.3 THz", J. Mol. Spetrosc., Vol. 170, 279–284 1995.

[11] V. L. Vaks, V. V. Khodos, and E. V. Spivak. "A Nonstationary Microwave Spectrometer", Review of Scientific Instruments, Vol. 70, Issue 8, pp. 3447–3453, August 1999.

[12] A. F. Krupnov and A. V. Burenin. "New Methods in Submillimeter Microwave Spectroscopy", Mol. Spectrosc: Mod. Research II, K. Narahar: Rao, ed. Academic Press, New York. (1976).

[13] Introduction to Extended Interaction Oscillators, Data Sheet 3445 5M 11/75, Varian Associates of Canada, Ltd. (Now CPI), Georgetown, Ontario, Canada, 1975.

[14] E. Alekseev and D. Pavlidis. "GaN-Based Gunn Diodes: Their Frequency and Power Performance and Experimental Considerations" www.eecs.umich.edu.

[15] www.virginiadiodes.com

[16] J. W. Dees. "Detection and Harmonic Generation in the Sub-Millimeter Wavelength Region", Microwave J., Vol. 9, pp. 48–55, 1966.

[17] K. M. Evenson, J. S. Wells, F. R. Petersen, B. L. Danielson, G. W. Day, R. L. Barger, and J. L. Hall, "Speed of Light from Direct Frequency and Wavelength Measurements of the Methane-Stabilized Laser", Phys. Rev. Lett. Vol. 29, 1346–1349 1972.

[18] R. E. Forsythe, V. T. Brady, and G. T. Wrixon. "Development of a 183 GHz Subharmonic Mixer", IEEE MTT-S International Microwave Symposium Digest, Orlando, FL, May 1978.

[19] R. W. McMillan, C. W. Trussell, Jr., R. A. Bohlander, J. C. Butterworth, R. E. Forsythe. "An Experimental 225 GHz Pulsed Coherent Radar", IEEE Trans. Microwave Theory and Techniques, Vol. 39, No. 3, pp. 555–562, March 1991.

[20] A. Vystavkin, D. Chouvaev, T. Claeson, D. Golubev, V., N. Kardashev, A., V. Kurt, L., M. Tarasov, A. Trubnikov, M. Willander. "Terahertz Andreev Reflection Based Normal Metal Hot-Electron Bolometer for the Cryogenic Telescope of the International Space Station", The 10th International Symposium on Space Terahertz Technology, Proceedings, pp 372–389, University of Virginia, March 16–18, 1999.

[21] "U3000 Uncooled Microbolometer Infrared Sensor", Data Sheet. The Boeing Company, Anaheim, CA, 1998.

[22] P. F. Goldsmith. Quasioptical Systems, IEEE Press, New York, 1997.

[23] J. M. Schuchardt, J. A. Stratigos, J. A. Gagliano, D. O. Gallentine, J. L. King. "Dual Frequency Multi-Channel Millimeter Wave Radiometers for High Altitude Observation of Atmospheric Water Vapor", 1979 MTT-S International Microwave Symposium Digest, pp. 540–542.

[24] P. F. Goldsmith, C.-T. Hsieh, G. R. Huguenin, J. Kapitzky, and E. L. Moore. "Focal Plane Imaging Systems for Millimeter Wavelengths", IEEE Trans. Microwave Theory and Techniques, Vol. 41, pp. 1664–1675, October 1993.

[25] www.army-technology.com/projects/apache/

[26] www.millivision.com

[27] Private Communication, Thermotrex Corporation, San Diego, CA.

[28] www.sae.org/aeromag/techupdate 12–99/05.htm

[29] http://www.st.northropgrumman.com/velocium/

[30] R. W. McMillan. "A Horizontal Atmospheric Temperature Sounder: Applications to Remote Sensing of Atmospheric Hazards", Int. J. Infrared and Millimeter Waves, Vol. 14, No. 5, pp. 931–948, 1993.

[31] E. Brown. University of California at Los Angeles, Private Communication, 2002.

[32] R. W. McMillan, Osborne Milton, Jr., M. C. Hetzler, R. S. Hyde, W. R. Owens. "Detection of Concealed Weapons Using Far-Infrared Bolometer Arrays", Proceedings of the 25th International Conference on Infrared and Millimeter Waves, Beijing, China, 12–15 September 2000.

[33] F. C. DeLucia. Ohio State University, Private Communication, 2004.

[34] K. R. Armstrong and F. J. Low. "Far-Infrared Filters Utilizing Small Particle Scattering and Antireflection Coatings", Applied Optics, Vol. 13, No. 2, pp. 425–430, February 1974.

[35] J. E. Peters and P. D. Ownby. “Far Infrared Transmission of Diamond Structure Semiconductor Single Crystals-Silicon and Germanium”, Optical Engineering, Vol. 38, No. 11, pp. 1924–1931, November 1999.